

# EFFICIENT POWER MANAGEMENT OF ENERGY SCAVENGERS FOR WIRELESS AUTONOMOUS SENSOR NETWORKS

Koray Karakaya<sup>1</sup>, Bert Op het Veld<sup>2</sup>, Ruud J.M. Vullers<sup>1</sup> and Valer Pop<sup>1</sup>

<sup>1</sup> Holst Centre/IMEC-NL, Eindhoven, the Netherlands

<sup>2</sup> Philips Research Laboratories, Eindhoven, the Netherlands

**Abstract:** The power chain of autonomous devices consists of an energy scavenger, power converter and energy storage system. The interaction between a piezoelectric vibration energy scavenger, the power converter and the energy storage system is investigated. A system level approach, including mechanical and electrical domains, is pursued for impedance matching from mechanical domain to electrical domain *and* from electrical domain to mechanical domain in order to investigate the physical design aspects of the energy scavenger on the electrical domain. Additionally, different battery and ultracapacitor systems are tested and their suitability for autonomous sensor networks is discussed in the paper.

**Key Words:** piezoelectric scavengers, power management, energy storage, impedance matching.

## 1. INTRODUCTION

Piezoelectric thin film stacks, ceramic and thick films, polymers and composites are widely investigated and used for energy scavenging applications [1]. Cost effective and reliable miniaturization of autonomous devices, higher integration to Si based microelectronic components makes thin film piezoelectric films and a micromachining approach for scavenger fabrication attractive. However, piezoelectric thin films generally exhibit high anisotropy due to preferential crystalline orientation and properties of thin films strongly depend on processing conditions. Therefore requires a mutual understanding of coupling of electrical and mechanical domains, with a perspective on material characteristics and geometrical aspects of scavengers.

Miniaturized energy harvesting devices will be key enablers for wireless autonomous transducer systems (WATS). An energy scavenger, in combination with an energy storage system (ESS), can be used to increase the energy efficiency of an autonomous system, thus extending the operational time of a fully autonomous energy storage-powered device [2]. The power distribution in a typical wireless autonomous system with a scavenger, ESS, sensor, processor and transceiver is shown in *Fig. 1*.

The power management module will convert the irregular energy flow generated by the scavenger into regulated energy, which meets the requirements for charging the energy storage system or directly to the autonomous sensor network node. In order to increase the efficiency

of the micropower module, a matching between the scavenger impedance and the load impedance is a must. Aspects regarding this impedance matching are discussed in this paper.

Various types of energy storage systems (ESS)

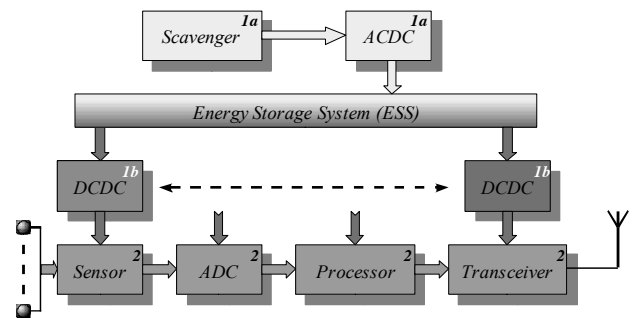


*Fig. 1: Typical power distribution in an autonomous sensor node from scavenger to load. The power distribution network is divided in a supply part (1a) for charging the EES and a load part (2a) to deliver the power to the functional circuits (2).*

exist on the market, *e.g.* batteries, ultracapacitors and fuel cells [2][3]. Different lithium (Li) battery and ultracapacitors systems are tested and their suitability for autonomous sensor networks is discussed.

## 2. PIEZOELECTRIC VIBRATION ENERGY SCAVENGERS

A typical piezoelectric scavenger, with a piezoelectric thin film stack on the cantilever with a seismic mass attached to that, is shown in *Fig. 2*. Voltage output of the piezoelectric stack operating in flexural mode (also called ‘31 mode’, referring to the principal axes) is proportional to the strain along the cantilever length *and* proportional to the bending amplitude of the cantilever structure.

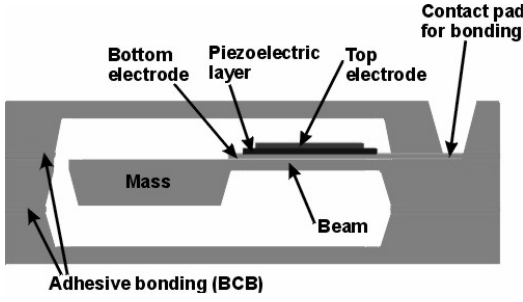


Fig.2: Schematic side view of the piezoelectric energy scavenger with a seismic mass.

The mass attached to the tip of the cantilever moves out-of-plane by external vibrations and causes tensile and compressive stress on the piezoelectric stack, which causes an alternating voltage. The amplitude of the voltage is proportional to the strain and may change depending on the amplitude of external vibrations. The energy harvested from the scavenger is extracted by a resistive load.

### 3. THE POWER CHAIN OF AN AUTONOMOUS DEVICE

The investigated power converter (Fig.3) has two major parts: First, the AC-DC converter, which rectifies the output voltage of the piezoelectric scavenger. The second part is a DC-DC converter charges the energy storage unit and supplies the load. Therefore, the power converter should be the optimal load for the scavenger for setting the scavenger to the maximum power point (MPP) and should be capable of charging the ESS in a well defined way.

#### 3.1. Maximum Power Point (MPP)

The linearized electrical equivalent circuit of the piezoelectric scavenger is given in Fig.4. In the figure, source voltage ( $V_s$ ), source inductance ( $L_m$ ), source capacitance ( $C_m$ ) and resistance  $R_m$  represent the mechanical quantities external force ( $F_{ext}$ ), mass ( $m$ ), stiffness of the beam ( $k$ ) and viscous damping ( $d$ ) and the capacitance of the piezoelectric stack ( $C_e$ ).

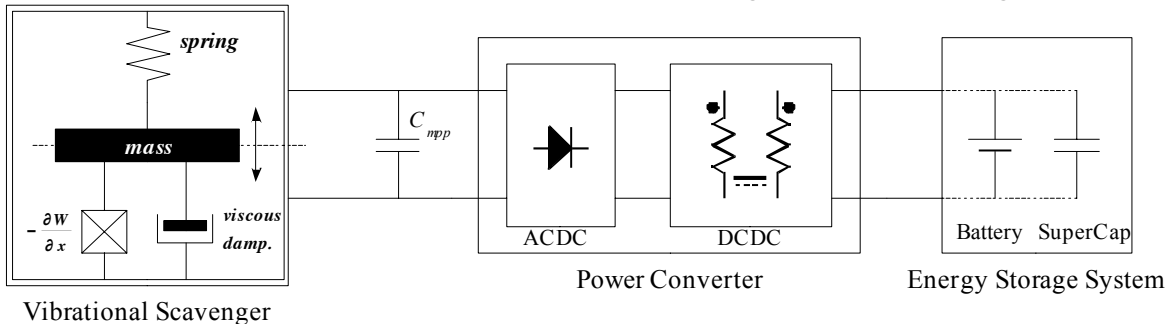


Fig. 3: Interaction between a piezoelectric scavenger, power converter and ESS.

The relation between the electrical equivalent and mechanical quantities is a function of the transformation ratio ( $\Gamma$ ) and given by following equations:

$$V_s = \frac{F_{ext}}{\Gamma}, L_m = \frac{m}{\Gamma^2}, C_m = k^{-1}\Gamma^2, R_m = \frac{d}{\Gamma^2} \quad (1-4)$$

where,  $\Gamma$  is a function of the piezoelectric coefficient and the piezoelectric coupling, which depends on the geometrical and mechanical aspects of the piezoelectric scavenger beam.

MPP of a system is a function of the voltage

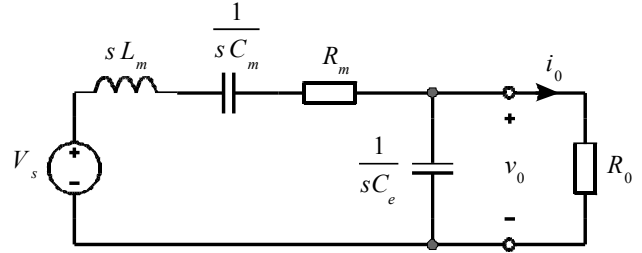


Fig.4: Electrical equivalent circuit of the piezoelectric scavenger.

source ( $V_s$ ), internal impedance ( $Z_s$ ) and the load impedance ( $Z_l$ ). MPP is achieved when the load impedance is equal to the conjugate of the internal impedance. In this case the maximum power output ( $P_{l,max}$ ) will be;

$$P_{l,max} = \frac{\left(\frac{1}{2}V_s\right)^2}{R_s} \quad (5)$$

The main approach for matching  $Z_l$  is using a resistive load ( $R_0$ ) and a parallel capacitance ( $C_0$ ), as shown in the parallel matching circuit presented in Fig.5.

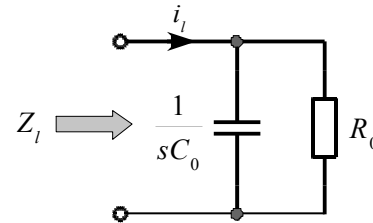


Fig. 5: Parallel matching network.

The minimum value of the  $C_0$  is equal to the capacitance of the piezoelectric stack, but can be enlarged by an external capacitor ( $C_{ext}$ ), if necessary. Substitution of  $Z_s$  and  $Z_l$  for impedance matching ( $Z_l=Z_s^*$ ) conditions:

$$Z_s = j\omega L_m + \frac{1}{j\omega C_m} + R_m \quad \hat{Z}_l = R_0 + \frac{1}{j\omega C_0} \quad (6-7)$$

The  $R_0$  and  $C_0$  for maximum power output can be extracted by solving Eq. 6 and Eq.7 for  $R_0$  and  $C_0$

$$R_0 = \frac{R_m^2 + \left( \omega L_m - \frac{1}{\omega C_m} \right)^2}{R_m} \quad (8)$$

$$C_0 = \frac{1}{\omega} \cdot \frac{\omega L_m - \frac{1}{\omega C_m}}{R_m^2 + \left( \omega L_m - \frac{1}{\omega C_m} \right)^2} \quad (9)$$

Matching of a resistor is possible since it corresponds to a positive value and conditions for  $R_0$  can always be fulfilled. However  $C_0$  matching depends on the following conditions related to the mechanical quality factor ( $Q_m$ ):

$$Q_m^2 \geq \frac{1}{2 + k_c - 2\sqrt{1 + k_c}} \text{ with } k_c = \frac{C_m}{C_0} \quad (10-11)$$

$$Q_m^2 = \frac{L_m}{R_m^2 C_m} \quad (12)$$

$L_m$ ,  $C_m$ ,  $R_m$  and  $C_0$  are depending on the scavenger dimensions and material properties like dielectric constant, piezoelectric constants and overall mechanical coupling. This means that the geometry of the scavenger and the material properties are crucial in order to reach to MPP.

#### 4. ENERGY STORAGE SYSTEMS

A performance analysis is necessary in order to test the various energy storage systems under an extended range of conditions. A test set-up has been designed containing the VMP3 automated energy storage tester [4], a computer and energy storage systems holders [2].

Three energy storage systems, *i.e.* two battery systems and one supercapacitor system have been selected for a first set of experiments. These experiments have been carried out in order to check the energy storage systems behaviour under the wireless autonomous sensor network (dis)charge C-rate (the charge/discharge current

normalized to the battery capacity) currents condition.

#### 4.1 Batteries

Two commercial, fresh and fully activated Li-ion batteries, *i.e.* Li<sub>1</sub> and Li<sub>2</sub>, from two different battery manufacturers were investigated. Since the batteries have a specified state of charge (SoC) upon delivery, the activation procedure performed at 25°C started with Constant-Current (CC) discharging at a 0.5 C-rate followed by two hours resting period [2].

The batteries were subjected to three standard Constant-Current Constant-Voltages (CCCV) and subsequent 0.5 C-rate discharge cycles, after which constant (dis)charge behaviour was attained. Standard charging was carried out with a constant maximum current at a 0.5 C-rate in the CC-mode until the maximum charge voltage of 4.2 V was attained in the subsequent CV-mode [3]. Evidently, the charging currents dropped in the CV-mode and charging was terminated at a predefined minimum current of a 0.05 C-rate, after which the battery has been considered fully charged. Discharging was terminated in this case when the cut-off cell voltage of 3.0 V was reached.

The most relevant test for a battery in a WATS node consists of pulse discharge steps. Therefore, after the activation measurements, pulse discharge measurements have been carried out. During these measurements the batteries have been firstly fully charged by applying the normal CCCV charging method. Furthermore, a pulse discharge step has been applied until the battery voltage reached the cut-off voltage level. The discharging has been considered at a 0.25 C-rate for 0.55 ms and 0.25 10<sup>-3</sup> C-rate for 4.05 ms. In this case, the pulse characteristics correspond with a possible WATS node load [2].

Fig. 6 shows the battery voltages during the pulse discharge of 'Li<sub>1</sub>' and 'Li<sub>2</sub>' batteries, where the upper and lower voltage values correspond with the 0.25 10<sup>-3</sup> and 0.25 C-rate current, respectively. It follows from Fig. 7 that the batteries show a different behaviour under the same discharging conditions. This can be explained by a different battery impedance and/or build-up of the overpotential [3]. In this case the Li<sub>1</sub> battery shows higher discharge efficiency

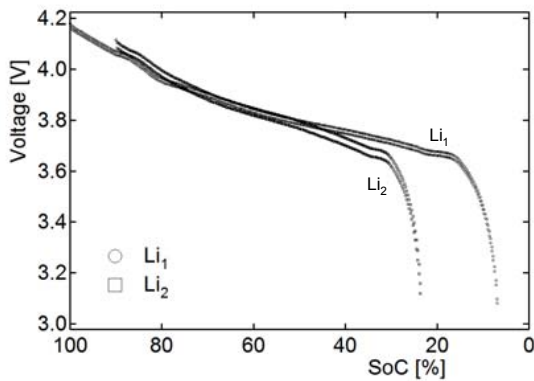


Fig.6. Discharge voltage curves measured under pulse discharging conditions for two different Li-ion batteries as function of SoC [%].

under the same pulse discharging conditions [3]. As a result, this battery will perform better in an autonomous sensor network.

#### 4.2 Ultracapacitors

A fresh and fully activated ultracapacitor has been considered in a second example. The activation procedure, performed at 25°C, started with Constant-Current (CC) discharging at a 0.5 C-rate followed by two hours resting period. Furthermore, three standards Constant-Current (CC) and subsequent 0.5 C-rate discharge cycles have been applied, after which constant (dis)charge behaviour was attained. Standard charging was carried out until the maximum charge voltage of 5 V was attained, after which the ultracapacitor has been considered fully charged, *i.e.* SoC = 100%. After a resting period of two hours, the ultracapacitor was discharged at a 0.5 C-rate. Discharging was terminated when the cut-off voltage of 0.1 V was reached [2].

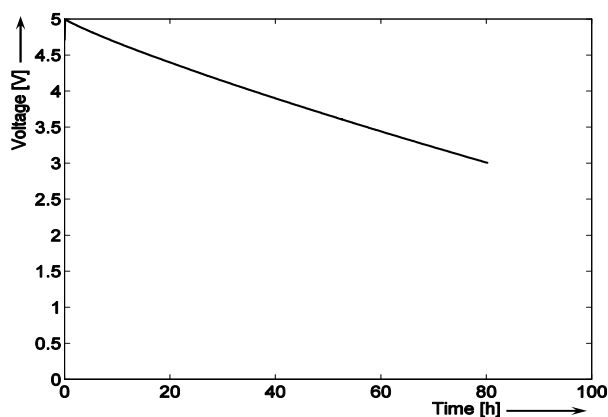


Fig. 7 The ultracapacitor self-discharge at a high SoC level as function of time [h].

In order to retrieve information about the ultracapacitor behaviour under different conditions self-discharge tests have been carried out at 25°C after a full CC charge step. The ultracapacitor voltage during equilibrium state [2] as function of the experiment time is plotted in Fig. 7.

It follows from Fig. 7 that the ultracapacitor self-discharge is of about 30% / 72 hours at high SoC levels. Consequently, the ultracapacitor may mainly be considered in an efficient and autonomous wireless sensor network as an energy buffer system.

#### 5. CONCLUSIONS

It has been showed that the  $Q_m$  is as critical as the other factor for impedance matching for achieving the MPP. Therefore the design of a piezoelectric energy scavenger should be considered in a system level approach for meeting the impedance matching requirements with reasonable values of inductance and capacitance.

Additionally, based on the presented results batteries are recommended as possible energy storage solutions in autonomous sensor networks. On the other hand, due to its low specific energy and high self-discharge rate the ultracapacitor systems are mainly recommended for applications where a large amount of power is needed for fractions of a second to several minutes.

#### REFERENCES

- [1] Anton, S.R. and Sodano H.A., A Review of Power Harvesting Using Piezoelectric Materials, *Smart Materials and Structures*, vol. 16, pp. R1-R21 (2007.)
- [2] V. Pop, R.J.M. Vullers, D. Hohlfield, T. Sterken, A. Schmitz, J. De Boeck, *Wireless Autonomous Transducer Solutions for Hybrid Electrical Vehicle Applications, Ecological Vehicles and Renewable Energies International Conference Monaco (2007)*
- [3] V. Pop, *Universal State-of-Charge Indication for Portable Applications*, Ph.D. thesis, University of Twente (2007)
- [4] BioLogic, VMP3 Multichannel Potentiostat/Galvanostat (2006)